Laboratory Investigation (2018) 98:609–619
https://doi.org/10.1038/s41374-017-0008-1

ARTICLE

Glutathione peroxidase 4 overexpression inhibits ROS-induced cell death in diffuse large B-cell lymphoma

Yuko Kinowaki[1] · Morito Kurata[1] · Sachiko Ishibashi[1] · Masumi Ikeda[1] · Anna Tatsuzawa[1,2] · Masahide Yamamoto[3] · Osamu Miura[3] · Masanobu Kitagawa[1] · Kouhei Yamamoto[1]

Received: 4 July 2017 / Revised: 15 October 2017 / Accepted: 23 October 2017 / Published online: 20 February 2018

Abstract

Regulation of oxidative stress and redox systems has important roles in carcinogenesis and cancer progression, and for this reason has attracted much attention as a new area of cancer therapeutic targets. Glutathione peroxidase 4 (GPX4), an antioxidant enzyme, has biological important functions such as signaling cell death by suppressing peroxidation of membrane phospholipids. However, few studies exist on the expression and clinical relevance of GPX4 in malignant lymphomas such as diffuse large B-cell lymphoma. In this study, we assessed the expression of GPX4 immunohistochemically. GPX4 was expressed in 35.5% (33/93) cases of diffuse large B-cell lymphoma. The GPX4-positive group had poor overall survival ($P = 0.0032$) and progression-free survival ($P = 0.0004$) compared with those of the GPX4-negative group. In a combined analysis of GPX4 and 8-hydroxydeoxyguanosine (8-OHdG), an oxidative stress marker, there was a negative correlation between GPX4 and 8-hydroxydeoxyguanosine ($P = 0.0009$). The GPX4-positive and 8-hydroxydeoxyguanosine-negative groups had a significantly worse prognosis than the other groups in both overall survival ($P = 0.0170$) and progression-free survival ($P = 0.0005$). These results suggest that the overexpression of GPX4 is an independent prognostic predictor in diffuse large B-cell lymphoma. Furthermore, *in vitro* analysis demonstrated that GPX4-overexpressing cells were resistant to reactive oxygen species-induced cell death ($P = 0.0360$). Conversely, GPX4-knockdown cells were sensitive to reactive oxygen species-induced cell death ($P = 0.0111$). From these data, we conclude that GPX4 regulates reactive oxygen species-induced cell death. Our results suggest a novel therapeutic strategy using the mechanism of ferroptosis, as well as a novel prognostic predictor of diffuse large B-cell lymphoma.

Introduction

Diffuse large B-cell lymphoma (DLBCL) is an aggressive subtype that accounts for one third of all newly diagnosed malignant lymphoma cases and over 80% of aggressive lymphomas [1]. DLBCL shows an aggressive behavior with a median survival of <1 year in untreated patients [1]. DLBCL includes a large number of disparate types distinguished by morphology, phenotype, gene expression profiles, and clinical outcomes [1]. Although there is an ongoing effort to classify DLBCL in order to treat by specific subtype [2], individual clinical course varies greatly. Therefore, it is becoming increasingly important to find new prognostic markers [3–5].

Tumor cells experience more oxidative stress than normal cells because of their high growth rate and higher oxygen requirement. To reduce oxidative stress, tumor cells develop various effective antioxidant systems, such as increased expression of the thioredoxin–thioredoxin

Supplementary information The online version of this article (https://doi.org/10.1038/s41374-017-0008-1) contains supplementary material, which is available to authorized users.

✉ Kouhei Yamamoto
yamamoto.pth2@tmd.ac.jp

[1] Department of Comprehensive Pathology, Graduate School of Medical and Dental Sciences, Tokyo Medical and Dental University, 1-5-45 Yushima, Bunkyo-ku, Tokyo 113-8510, Japan

[2] Department of Analytical Information of Clinical Laboratory Medicine, Graduate School of Health Care Science, Bunkyo Gakuin University, 1-19-1, Mukougaoka, Bunkyo-ku, Tokyo, Japan

[3] Department of Hematology, Graduate School of Medical and Dental Sciences, Tokyo Medical and Dental University, 1-5-45 Yushima, Bunkyo-ku, Tokyo 113-8510, Japan

reductase system [6] and the cystine/glutamic acid transporter (xc^-) system [7, 8]. These antioxidant systems and related molecules are essential for cancer progression and are hence targeted by anticancer drugs and used as biomarkers in a variety of cancers [9–11].

Glutathione peroxidase (GPX) is an intracellular antioxidant enzyme responsible for reducing peroxidized phospholipids. The GPX family member GPX4, also known as phospholipid-hydroperoxide glutathione peroxidase, is considered one of the most important antioxidant enzymes in mammals [12–14]. Recently, there have been reports suggesting that overexpression or depletion of GPX4 is responsible for tumorigenesis and tumor progression [15–21]. However, the frequency of GPX4 expression in malignant lymphoma including DLBCL, its histological relevance, and its relevance prognosis are not currently known.

In the present study, we clarify that GPX4 overexpression contributes to poor prognosis in DLBCL via inhibition of reactive oxygen species (ROS)-induced cell death by clinicopathologic study and in vitro cell death analysis.

Materials and methods

Patients and pathological specimens

We examined pathological specimens obtained from 93 patients with DLBCL at Tokyo Medical and Dental University Hospital, Tokyo, between 2000 and 2014. Of the 93 patients, 47 received R-CHOP (rituximab, cyclophosphamide, doxorubicin, vincristine, and prednisolone) therapy, and 46 received CHOP therapy as induction therapy. Pathologic diagnosis was confirmed according to the WHO criteria by two pathologists (KY and MK). Specimens were obtained by biopsy or surgical resection, fixed in 10 % neutralized formalin, and embedded in paraffin according to routine protocols for conventional histopathological examination. Informed consent was obtained from all patients, and the study was approved by the ethics committees of Tokyo Medical and Dental University. All procedures were performed in accordance with the ethical standards established by these committees (M2000-1818).

Immunohistochemistry

Formalin-fixed, paraffin-embedded tissue was sliced at a thickness of 4 μm, and the sections were placed on silane-coated slides and deparaffinized. Heat-based antigen retrieval, endogenous peroxidase blockade using 3% hydrogen peroxide, and blocking were performed with normal sera. The primary antibodies used were GPX4, 8-OHdG (15A3), CD20, CD10, bcl-6, and MUM-1 (Table 1). The specimens with primary antibodies were incubated overnight at 4 °C. Primary antibodies were detected using an ABC Kit (Vector Laboratories, Burlingame, CA, USA) for 8-OHdG, CD20, CD10, and MUM-1 and Novolink Polymer Detection Systems (Leica, Wetzlar, Germany) for GPX4 and bcl-6. The color development was performed using diaminobenzidine (DAB; Nichirei Bioscience, Japan) or the HISTOFINE simple stain AP series (Nichirei Bioscience). Immunohistochemical expression of CD20 was used for diagnosis of DLBCL, and CD10, bcl-6, and MUM-1 were used to classify DLBCL into germinal center B (GCB) and non-GCB groups according to Hans algorithm [22]. For double immunostaining, heat treatment and blocking were performed between each step, and detection was performed using HISTOFINE simple stain AP series with Vector Blue (Vector Laboratories) or Novolink Polymer Detection Systems with DAB.

Preparation of RNA and quantitative reverse transcriptase polymerase chain reaction (qRT-PCR) for DLBCL tissue sample

RNA was extracted from fresh-frozen DLBCL samples using an RNeasy Mini Kit (Qiagen, Hilden, Germany), and reverse transcriptase reaction was performed using TaqMan

Table 1 Kinowaki et al. Summary of immunohistochemistry reagent combinations used in this study

Antibody	Host	Type	Clone	Source	Dilution
GPX4	Rabbit	Monoclonal	EPNCIR144	Abcam[a]	1:250
8-OHdG (15A3)	Mouse	Monoclonal	SC-66036	Santa Cruz[b]	1:2000
CD20	Mouse	Monoclonal	L26	Agilent[c]	1:1
CD10	Mouse	Monoclonal	56C6	Leica[d]	1:100
bcl-6	Mouse	Monoclonal	PG-B6p	Agilent[c]	1:100
MUM-1	Mouse	Monoclonal	MUM1p	Agilent[c]	1:500

[a] Abcam, Cambridge, MA, USA.

[b] Santa Cruz Biotechnology, Inc., Dallas, TX, USA.

[c] Agilent, Santa Clara, CA, USA.

[d] Leica Biosystems, Wetzlar, Germany

Reverse Transcription Reagents (Thermo Fisher Scientific, Waltham, MA, USA) N808-0234. Real-time PCR was performed using THUNDERBIRD SYBR qPCR Mix TOYOBO QPS-201 (TOYOBO, Tokyo, Japan) and ABI Prism 7900HT Sequence Detection System (Applied Biosystems, Foster, CA, USA). Primer sequences for *GPX4* were 5′-CTGCTCTGTGGGGCTCTG-3′ and 5′-ATGT CCTTGGCGGAAAACTC-3′, and for GAPDH, endogenous control gene for normalization, 5′-ACAGTCAGCCG CATCTTCTT-3′ and 5′-AATTTGCCATGGGTGGAAT-3′. Values for each gene expression were normalized using the relative quantity of β-actin as an endogenous control.

Clinicopathologic analysis

As clinicopathologic factors, a total of ten parameters were analyzed as follows: age (≥65 vs. <65 years), gender (male vs. female), Ann Arbor status (stage I, II vs. III, IV), lactate dehydrogenase (normal; <240 IU/l vs. elevated; ≥240 IU/l), performance status (0–1 vs. 2–4), International Prognostic Index (IPI) score (0–2 vs. 3–5), B symptoms (yes vs. no), the number of extranodal site (0 vs. ≥1), bone marrow involvement (yes vs. no), and Hans algorithm (GCB vs. non-GCB type).

Cell lines and culture

The LCL-K cell line obtained from human peripheral blood B cells with Epstein–Barr virus infection was established at the Department of Hematology, Graduate School of Medical and Dental Sciences, Tokyo Medical and Dental University, Tokyo, Japan [23]. The cells were cultured in RPMI-1640 medium with L-glutamine and phenol red (Wako Pure Chemical Industries, Ltd., Osaka, Japan) containing 10% fetal bovine serum and 1% penicillin–streptomycin solution. Cells were passaged at a ratio of 1:5–1:8 every 2–3 days.

Establishment of GPX4-overexpressing LCL-K cell line using recombinant lentiviruses and lentiviral transduction

Human GPX4, 3× FLAG, and 3′-UTR of GPX4 were subcloned using Raji cell cDNA and 3× FLAG control vector. They were subsequently inserted into mammalian expression vectors containing the cytomegalovirus promoter (Sigma-Aldrich, St. Louis, MO, USA). The *GPX4* gene with attB sites was amplified by PCR using the Expand High Fidelity PCR System (Roche Diagnostics, Somerville, NJ, USA). The fragment was then transferred to the pENTR vector via the Invitrogen Gateway BP Clonase reaction and then transferred to pLenti-PGK-DEST-pgk-Hygro via the Invitrogen Gateway LR Clonase reaction (Thermo Fisher Scientific), following the manufacturer's instructions. GPX4-overexpressing LCL-K (LG) cells were established, and GPX4 mRNA and protein overexpression were confirmed by qRT-PCR and western blot, respectively. The intensity of western blot bands was quantified by densitometry with Image Lab 4.1 Software (Bio-Rad Laboratories, Hercles, CA, USA). Four monoclones were obtained from each cell line of LG (LG-1, LG-2, LG-3, and LG-4) and control LCL-K cells (LC; LC-1, LC-2, LC-3, and LC-4) by limiting dilution.

Establishment of GPX4-knockdown LCL-K cell line by lentiviral shRNA silencing of GPX4

GPX4 shRNA lentiviral vector was constructed by annealing two oligonucleotides (forward primer, 5′- GA TCTCGGCACATGGTTAACCTGGAGCTTCCTGTCAC TCCAGGTTAACCATGTGCCTTTTTTA-3′, and reverse primer, 5′- AGCTTAAAAAAGGCACAGGTTAACCTG GAGTGACAGGAAGCTCCAGGTTAACCATGTGCCG A-3′) pretreated at 95 °C for 5 min and gradually cooled down to room temperature. The annealed products were cloned into pSUPER driven by a human H1 promoter, and the GPX4-silenced LCL-K cell line was generated after puromycin selection. GPX4 knockdown was confirmed at the mRNA level by qRT-PCR and at the protein level by western blot.

ROS detection by flow cytometry in LG and LC cells

To detect intracellular ROS in LCL-K cells, CellROX Deep Red Reagent (Thermo Fisher Scientific) was used. This reagent freely enters the cells and becomes highly fluorescent after being oxidized by ROS [24, 25]. GPX4-overexpressing LCL-K cells and control vector-transfected LCL-K cells were seeded at a density of 2×10^5 cells/well in a 24-well culture plate with 500 µl media/well and treated with 20 µM tert-butyl hydroperoxide (TBHP), a major inducer of oxidative stress [26, 27], for 6 h. As a negative control, 500 mM N-acetylcysteine (NAC) was pretreated and incubated for 1 h. After TBHP and NAC treatment, the medium was discarded, and cells were washed with phosphate-buffered saline (PBS). Subsequently, the cells were incubated with 1 µM CellROX Deep Red Reagent for 30 min at 37 °C, and the cultures were analyzed by flow cytometry.

Assessment of cell viability upon treatment of LCL-K cells with TBHP and etoposide

LCL-K cell viability upon treatment with TBHP and etoposide was analyzed using the following methods. The cells were seeded at a density of 2×10^5 cells/well in a 24-well culture plates with 500 µL media/well and treated with 20

μM TBHP for 6 h and 250 nM etoposide for 24 h. After treatment with TBHP or etoposide, the medium was discarded and the cells were washed with PBS. Propidium iodide was added to each well and incubated at 37 °C in the dark for 10 minutes. The samples were then analyzed by flow cytometry by a BD FACSCanto II analyzer (Becton Dickinson and Company, Franklin Lakes, NJ, USA).

Statistical analysis

Correlations between the two groups were determined with the χ^2-test and Fisher's exact test. Overall survival (OS) duration was calculated from the date of diagnosis to the date of last follow-up or death. Progression-free survival (PFS) duration was calculated from the date of diagnosis to the time of progression or death. Kaplan–Meier survival curves were used to estimate OS and PFS rates, and the log-rank test was used to assess differences in survival between groups. Univariate and multivariate analyses were performed with the Cox proportional hazard regression model. Mann–Whitney's *U*-test was used to evaluate the difference in the analysis of mRNA expression by qRT-PCR. The Student's *t*-test was used to determine the statistical significance of western blot band intensity or qRT-PCR expression. All differences with a $P \leq 0.05$ were considered statistically significant. Ekuseru-Toukei version 1.15 (Social Survey Research Information Co., Ltd, Tokyo, Japan, 2012) was used for all the analyses.

Results

GPX4 and 8-OHdG immunohistochemistry in patients with DLBCL and assessment of positive cells

To evaluate GPX4 expression in DLBCL, we performed immunostaining (Fig. 1a, b). The DLBCL cases were

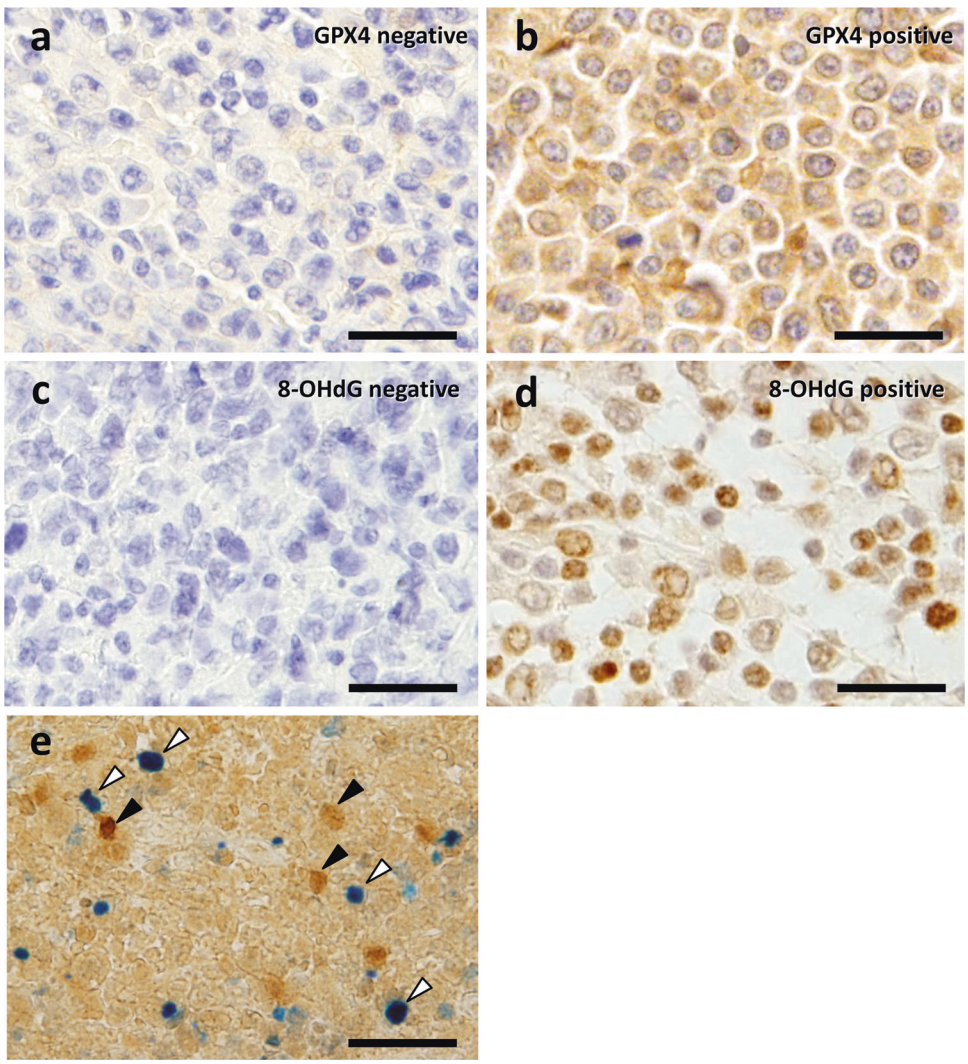

Fig. 1 Representative images of GPX4 and 8-OHdG immunohistochemistry in cases of DLBCL. Formalin-fixed paraffin-embedded tissue sections were used for immunohistochemical staining of GPX4 **a**, **b** and 8-OHdG **c**, **d**. All images are shown at × 400 magnification. Scale bars, 20 μm. **a** A case of DLBCL showing negative staining for GPX4. **b** A case of DLBCL showing cytoplasm staining for GPX4 in most tumor cells. **c** A case of DLBCL showing negative staining for 8-OHdG. **d** A case of DLBCL showing nuclear staining for 8-OHdG in more than half of the tumor cells. **e** Double immunostaining for GPX4 (brown) and 8-OHdG (blue) in DLBCL samples. Black arrowheads indicate GPX4-positive DLBCL cells. White arrowheads indicate 8-OHdG-positive DLBCL cells. GPX4 and 8-OHdG expression was mutually exclusively

Table 2 Patient characteristics as stratified by GPX4 status

Characteristics	GPX4		*P*-values
	Positive	Negative	
Age			
≥65 y	24	29	0.0292
<65 y	9	31	
Gender			
Male	18	41	0.2605
Female	15	19	
Ann Arbor status			
I, II	19	33	0.8309
III, IV	14	27	
LDH[a]			
Normal	11	24	0.6554
Elevated	22	36	
Performance status			
0–1	20	41	0.4986
2–4	13	19	
IPI score[b]			
0–2	20	45	0.1635
3–5	13	15	
B symptoms			
Yes	14	17	0.1775
No	19	43	
Extranodal site			
0	12	21	1.0000
≥1	21	39	
Bone marrow involvement			
Yes	9	6	0.0406
No	24	54	
Hans algorithm			
GCB[c]	21	38	1.0000
Non-GCB	12	22	

[a] LDH: lactate dehydrogenase.

[b] IPI: International Prognosis Index.

[c] GCB: germinal center B cell

classified as GPX4-positive or GPX4-negative. To qualify as GPX4-positive, at least 50% of the DLBCL cells were required to test positive for GPX4 in the immunohistochemistry assay. Of the 93 patients, 33 cases (35.5%) were GPX4-positive. GPX4 protein was detected in the cytoplasm of the DLBCL cells.

8-OHdG is known as an end product of oxidative damage to DNA and known to be a sensitive oxidative stress biomarker. 8-OHdG expression was considered positive when >50% of the DLBCL cells in a specimen were stained. In our study, 27 out of 68 evaluated cases (39.7%) were positive for 8-OHdG, which was expressed in the nucleus of the DLBCL cells (Fig. 1c, d). Double immunostaining of GPX4 and 8-OHdG revealed that their expression was mutually exclusive (Fig. 1e).

Expression analysis of GPX4 mRNA in DLBCL

To determine whether GPX4 is overexpressed at the protein level or at the mRNA level in DLBCL, we first evaluated the GPX4 protein expression level in 48 DLBCL cases by immunohistochemistry and, depending on the results, divided into two groups, GPX4-positive and GPX4-negative group, according to the criteria described above. We then performed qRT-PCR to measure mRNA expression level using frozen samples of DLBCL. As shown in Supplementary Data 1, there was no significant differences in *GPX4* mRNA between GPX4-positive and GPX4-negative groups ($P = 0.4433$).

Clinical significance of GPX4 overexpression in DLBCL

To evaluate the relationship between clinical outcome and GPX4 expression in DLBCL, various clinical features were investigated. GPX4 positivity was significantly correlated with age ($P = 0.0292$), and bone marrow involvement ($P = 0.0406$) (Table 2). The staining patterns did not differ by patient gender, Ann Arbor staging classification, lactate dehydrogenase, performance status, IPI score, B symptoms, extranodal site, or Hans algorithm.

GPX4-positive group showed poor prognosis in OS/PFS

We next investigated the correlation between GPX4 positivity and patient prognosis. Kaplan–Meier analysis revealed that the GPX4-positive group had significantly worse OS (Fig. 2a, $P = 0.0032$) and PFS (Fig. 2b, $P = 0.0004$) than the GPX4-negative group.

We then tested 10 parameters, including age, gender, Ann Arbor stage, lactate dehydrogenase, performance status, B symptom, extranodal site, bone marrow involvement, Hans algorithm, and GPX4 expression by multivariate analysis using the Cox proportional hazard model (Table 3). We found that the performance status 2–4 (vs. performance status 0–1, hazard ratio 4.5595, $P = 0.0034$) and GPX4-positivity (vs. GPX4-negativity, hazard ratio 4.5345, $P = 0.0009$) independently predicted shorter OS.

Inverse correlation between GPX4 and 8-OHdG expression

In order to test the hypothesis that GPX4-expressing DLBCL cells show less-intracellular ROS accumulation, we analyzed the correlation between GPX4 and 8-OHdG

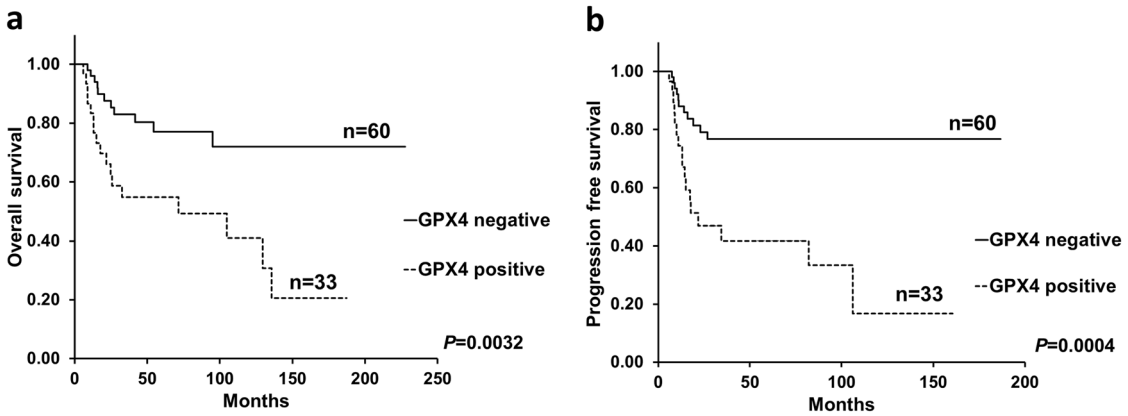

Fig. 2 GPX4-positive group shows poor prognosis in OS/PFS. **a** Kaplan–Meier analysis shows that the GPX4-positive group had a significantly worse OS ($P = 0.0032$) than GPX4-negative group. **b** Kaplan–Meier analysis shows that the GPX4-positive group had a significantly worse PFS ($P = 0.0004$) than GPX4-negative group

expression immunohistochemically. There was a significant inverse correlation between GPX4 and 8-OHdG positivity ($\chi^2 = 11.013$, df = 1, $P = 0.0009$) (Table 4). Next, to analyze whether this combination of GPX4 and 8-OHdG expression predicts patient prognosis, we built survival curves (Kaplan–Meier analysis, Fig. 3). Patients with DLBCL were divided into four subgroups as follows: GPX4-negative and 8-OHdG-negative group, GPX4-negative and 8-OHdG-positive group, GPX4-positive and 8-OHdG-negative group, and GPX4-positive and 8-OHdG-

Table 3 Univariate and multivariate analyses of clinicopathological factors influencing overall survival

Variable	Category	Number of patients	*P*-value by log-rank test	HR[a]	95% CI[b]	*P*-value by Cox proportional hazards
Age	≥65y	53	0.6654			
	<65y	40				
Gender	Male	59	0.6266			
	Female	34				
Ann Arbor stage	I, II	52	0.0030	0.8535	0.2071–3.5181	0.8265
	III, IV	41				
LDH[c]	Normal	35	0.0166	1.3538	0.4691–3.9068	0.5754
	Elevated	58				
Performance status	0–1	61	<0.0001	4.5595	1.6516–12.5875	0.0034
	2–4	32				
B symptoms	Yes	31	<0.0001	2.4129	0.9075–6.4152	0.0775
	No	62				
Extranodal site	0	33	0.0690			
	≥1	60				
Bone marrow involvement	Yes	15	0.0016	1.5652	0.5611–4.3662	0.3921
	No	78				
Hans algorithm	GCB[d]	59	0.8615			
	Non-GCB	34				
GPX4	Positive	33	0.0002	4.5345	1.8538–11.0914	0.0009
	Negative	60				

[a] HR: Hazard ratio.

[b] CI: Confidence Interval.

[c] LDH: Lactate dehydrogenase.

[d] GCB: Germinal center B cell

Table 4 Frequency table GPX4 versus 8-OHdG

8-OHdG	GPX4		
	Positive		Negative
Positive	8		29
Negative	21		14
	Chi-square test		
	χ^2	df	*P*-value
Pearson Chi-square	11.01308	1	0.0009

The frequency of GPX4-positive cases was significantly correlated with that of 8-OHdG-positive cases by Pearson Chi-square test ($\chi^2 = 11.01308$, $df = 1$, $P = 0.0009$)

positive group. The GPX4-positive and 8-OHdG-negative group showed the worst prognosis, though there were no significant differences between the four subgroups in both OS and PFS (Fig. 3a and b). Subsequently, we divided patients into two groups: the GPX4-positive and 8-OHdG-negative group and all remaining patients. The GPX4-positive and 8-OHdG-negative group showed significantly poorer prognosis than the other groups, in both OS ($P = 0.0170$, Fig. 3c) and PFS ($P = 0.0005$, Fig. 3d).

Expression of GPX4 regulates ROS-induced cell death in LCL-K cell

Based on the finding that GPX4 overexpression in DLBCL correlated with poor patient prognosis and negatively correlated with intracellular ROS accumulation as determined by 8-OHdG staining, we hypothesized that overexpression induces resistance of tumor cells to ROS-induced cell death. Accordingly, reducing GPX4 expression should sensitize cells to ROS-induced death. To test this hypothesis, we used in vitro systems. We established LG and LC cells by transfection with a lentiviral vector (Fig. 4a). Overexpression of GPX4 in LG cells was detected at the mRNA level by qRT-PCR (Fig. 4b) and at the protein level by western blot (Fig. 4c and d). We then measured the difference in accumulation of ROS between LG and LC cells under treatment with TBHP by flow cytometry using CellROX Deep Red Reagent. The fluorescent signal was less intense in LG-1 than in LC-1, indicating that LG-1 had less-intracellular ROS accumulation than LC-1. Thus, GPX4 overexpression inhibited the accumulation of intracellular ROS (Fig. 4e). We then measured viability of cells treated with etoposide or TBHP to LG monoclones (LG-1, LG-2, LG-3, and LG-4) and LC monoclones (LC-1, LC-2, LC-3,

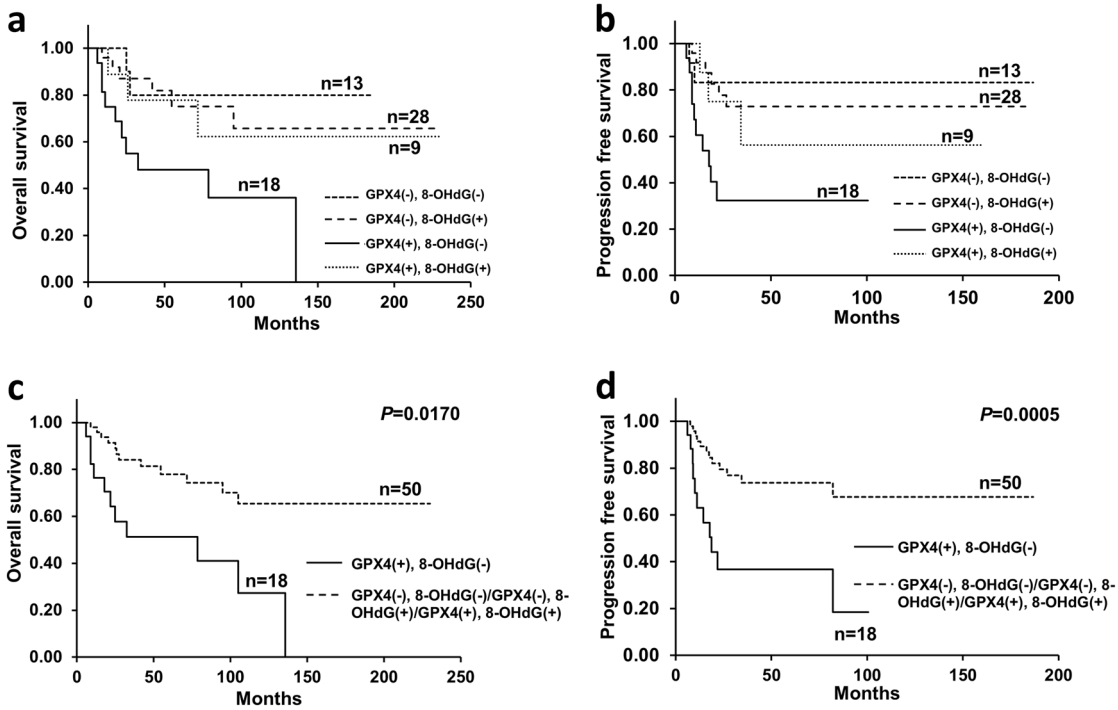

Fig. 3 Inverse correlation between GPX4 and 8-OHdG expression. **a** GPX4-positive and 8-OHdG-negative groups show the worst prognosis, though there were no significant differences in OS between the four subgroups. **b** GPX4-positive and 8-OHdG-negative groups show the worst prognosis, though there were no significant differences in PFS between the four subgroups. **c** GPX4-positive and 8-OHdG-negative groups show significantly poorer prognosis in OS than the other groups ($P = 0.0170$). **d** GPX4-positive and 8-OHdG-negative groups show a significantly poorer prognosis in PFS than the other groups ($P = 0.0005$)

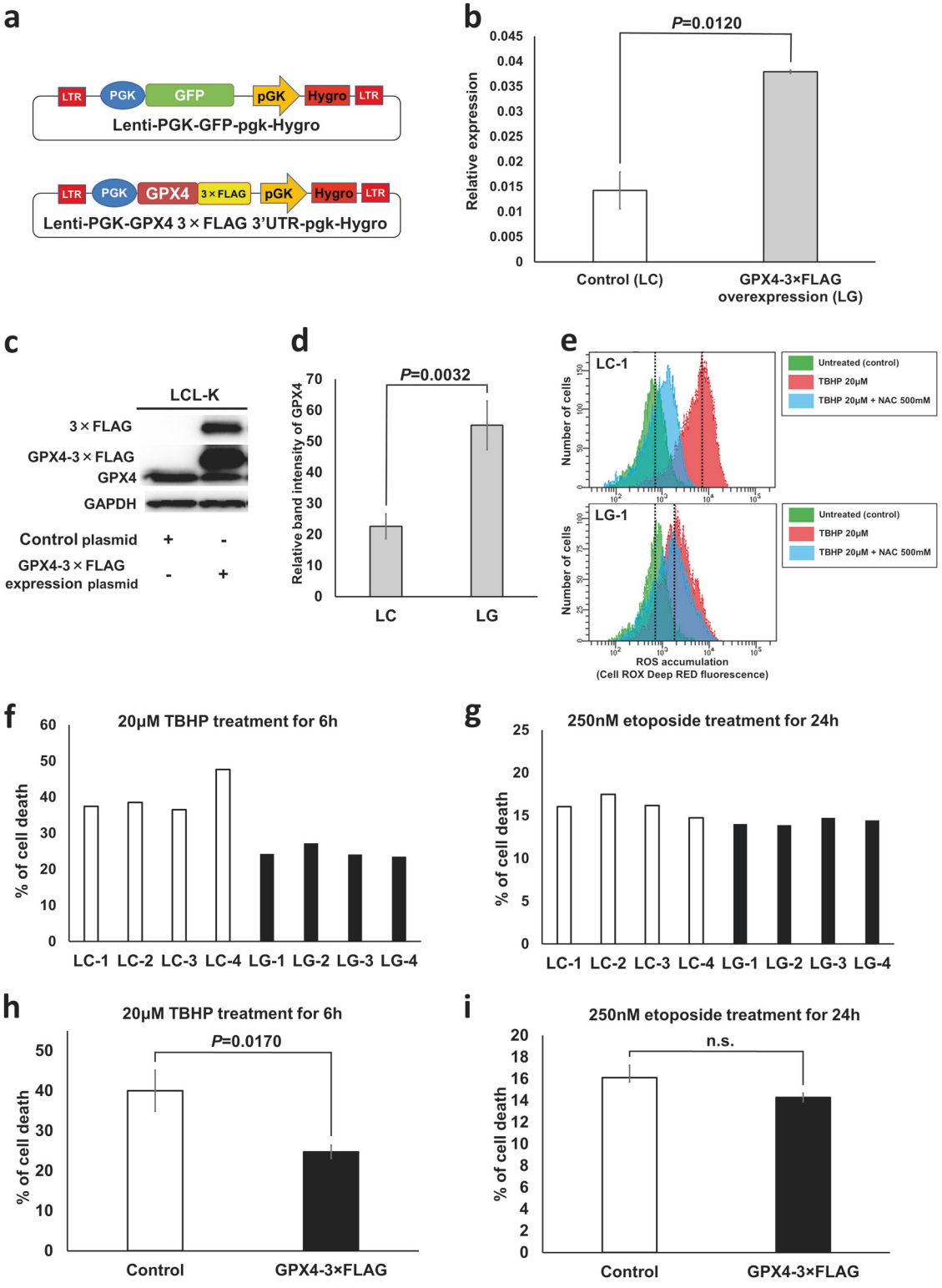

and LC-4) (Fig. 4f and g). The mean cell death rate was significantly suppressed in LG compared with LC cells after treatment with TBHP ($P = 0.0170$, Fig. 4h), but it was not significantly different after treatment with etoposide ($P = 0.1481$, Fig. 4i).

We established a GPX4-knockdown cell line by lentiviral shRNA silencing of GPX4. Knockdown efficiency of GPX4 at the mRNA level was quantified by qRT-PCR (Fig. 5a; $P = 0.0306$) and at the protein level by western blot (Fig. 5b and c). We measured cell viability upon

◀ **Fig. 4** Overexpression of GPX4 inhibits ROS-induced cell death in LCL-K cells. **a** Schematic representation of lentiviral vector constructs for the control vector (top) and GPX4-3 × FLAG vector (bottom). LTR, long terminal repeat; PGK, phosphoglycerate kinase promoter; Hygro, hygromycin-resistant gene; GFP, green fluorescent protein. **b** qRT-PCR shows a significant overexpression in GPX4 at the mRNA level in LG cells ($P = 0.0120$). **c** Overexpression of GPX4 in LG cells was detected at the protein level by western blot. **d** Densitometry analysis shows a significant increase in GPX4 blot band intensity in LG cells ($P = 0.0032$). **e** ROS detection by flow cytometry in LC-1 (top) and LG-1 (bottom) cells using fluorescent dye CellROX Deep Red Reagent. Compared with LC-1 cells, LG-1 cells show a decrease in staining with the CellROX Deep Red Reagent after treatment with 20 μM TBHP (red), which means lower intracellular ROS level in LG-1 than in LC-1 cells. Untreated control cells are shown in green, and cells pretreated with NAC before treatment with TBHP are shown in blue. **f** Cell viability analysis of LC and LG clones upon treatment with 20 μM TBHP for 6 h. LC-1, LC-2, LC-3, and LC-4 are monoclones of LC. LG-1, LG-2, LG-3, and LG-4 are monoclones of LG; LC, control LCL-K cell; LG, GPX4-overexpressing LCL-K cell. **g** Cell viability analysis of LC and LG clones upon treatment with 250 nM etoposide for 24 h. **h** Mean cell death rate was significantly suppressed in LG cells compared with LC cells after treatment with TBHP ($P = 0.0170$). **i** Mean cell death rate was not significantly different between LG and LC cells after treatment with etoposide ($P = 0.1481$); n.s., non-significant

treatment with etoposide and TBHP and found that cell death rate was significantly increased in GPX4-knockdown LCL-K cells compared with that of control LCL-K cells after treatment with TBHP ($P = 0.0111$, Fig. 5d). However, no significant difference was detected after treatment with etoposide ($P = 0.1574$, Fig. 5e).

Discussion

GPX4, a selenoprotein and an intracellular antioxidant, is the only antioxidative enzyme that can directly reduce phospholipid hydroperoxides generated in biological membranes. It has an important role in oxidative homeostasis. It is known to show several different modes of intracellular localization: to the cytoplasm (cGPX4), mitochondria (mGPX4), and nucleolus (nGPX4) [28]. In normal somatic cells, expression level of the cGPX4 protein is ten times higher than that of mGPX4, and the expression level of nGPX4 is very low [29].

Deficiency in GPX4 is reported to be associated with fetal death, male infertility, and hepatic and cardiac cell death in mice [14, 30]. Almost all normal mammalian cells show GPX4 activity, particularly abundant in testis, adipose tissue and retina [30, 31]. However, GPX4 is hardly detectable in lymphocytes by immunohistochemistry [32] and has decreased expression at the mRNA level [21], though its enzymatic activity is detected to some extent [33].

Although there are few reports of GPX4 in tumor tissue, GPX4 was found to be increased in colon carcinomas [15] and in hepatocellular carcinomas [16], and decreased GPX4 level has been reported in pancreatic cancer [17], breast cancer cells [18], clear cell renal cell carcinomas [19], and gastric cancer [21]. A variant of the gene encoding GPX4 has been reported to influence prostate cancer risk [20]. Despite these reports, there is yet no consensus on the expression and role of GPX4 in tumors. To the best of our knowledge, no study has yet assessed the relationships between GPX4 expression and patient prognosis in malignant lymphoma. However, we show here that there was no significant difference in mRNA level between the GPX4-positive group and GPX4-negative group, which suggests that post-transcriptional regulation, such as the ubiquitin-proteasome system, may be involved in the expression of GPX4 protein in malignant lymphoma, including DLBCL.

In this study, 33/93 DLBCL cases were positive for GPX4, which was overexpressed compared with non-neoplastic B cells. The GPX4-positive group showed significantly poorer prognosis in OS and PFS. Moreover, GPX4 overexpression was an independent prognostic predictor. These results suggest that GPX4 overexpression might result in poor prognosis by a different mechanism than the existing prognostic predictors of DLBCL. It is possible that we only detected cytoplasmic GPX4 because of its abundant endogenous distribution compared with that of mitochondrial or nucleolus GPX4. However, cytoplasmic positivity of GPX4 might suggest the importance of cytoplasmic GPX4 in particular in tumor cell survival; Imai et al. [30] reported that only cytoplasmic GPX4 knockout results in embryonic lethality in mice . Considering that LCL-K cells demonstrated resistance to cell death after treatment with TBHP, which is ROS generator, but not after treatment with etoposide, which is known as nucleolus stressor [34], GPX4-overexpressing tumor cells are likely to acquire the ability to neutralize ROS and thus combat oxidative stress. Overexpression of redox-regulating enzymes such as thioredoxin and glutamate–cysteine ligase in patients with DLBCL has been reported to lead to poor prognosis owing to the ability of tumor cells to cope with oxidative stress from ROS-generating anticancer drugs such as doxorubicin, vincristine, and cyclophosphamide [35].

However, the exact roles of oxidative stress and the antioxidants that detoxify in cancer progression have been controversial, because oxidative stress can promote or suppress tumor development in different contexts [36]. Partly owing to the complexity of the relationships between oxidative stress and the redox system, there is no consensus on the relationship between aberrant expression of GPX4 and patient prognosis in human tumors. Nevertheless, there are relatively more reports showing that high expression of redox enzymes in tumor cells leads to poor prognosis [37, 38].

Recently, Yang et al. [39] proposed a non-apoptotic form of cell death called ferroptosis that can be triggered by inactivation of GPX4 or depletion of intracellular

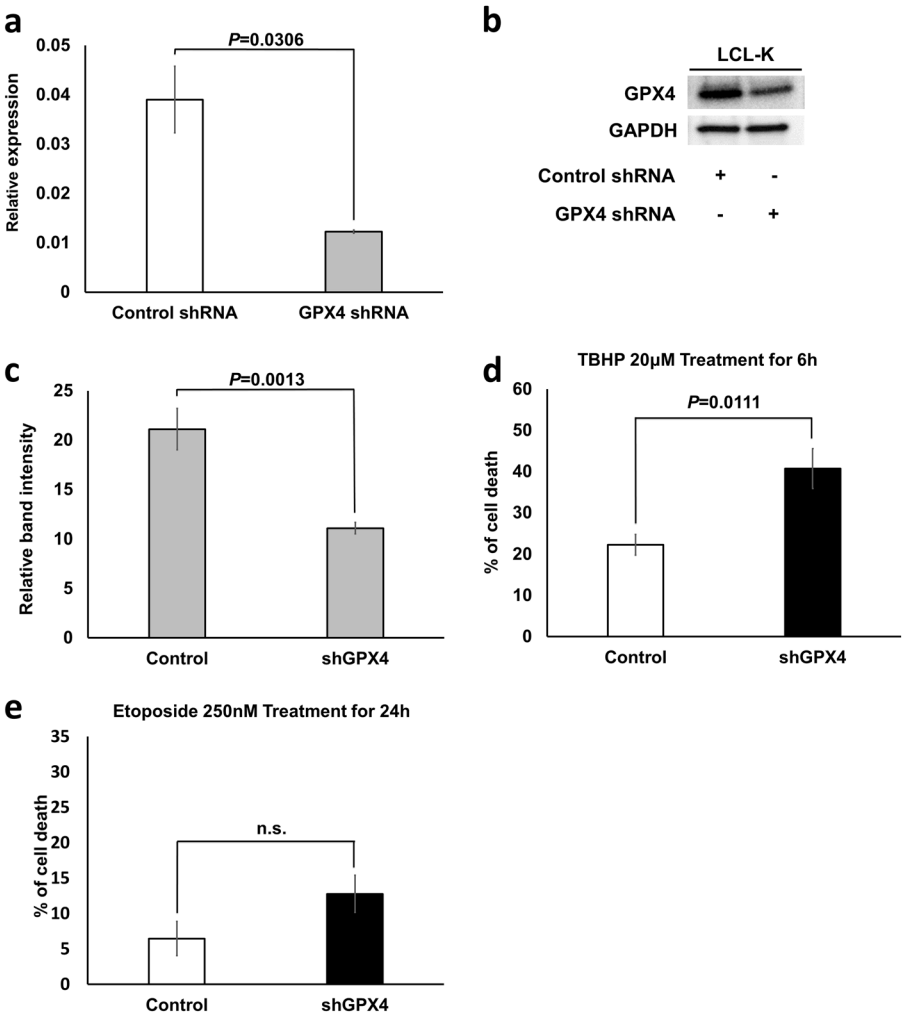

Fig. 5 GPX4 knockdown promotes ROS-induced cell death in LCL-K cells. **a** Knockdown efficiency of GPX4 was detected at the mRNA level by qRT-PCR. GPX4 mRNA expression level was significantly decreased in GPX4-knockdown LCL-K cells ($P = 0.0306$). **b** Knockdown efficiency of GPX4 was detected at the protein level by western blot. **c** Densitometry analysis shows that GPX4 band intensity was significantly decreased in GPX4-knockdown LCL-K cells ($P = 0.0013$). **d** Cell death rate was significantly increased in GPX4-knockdown LCL-K cells compared with that of control LCL-K cells after treatment with TBHP ($P = 0.0111$). **e** Mean cell death rate was not significantly different between LG and LC cells after treatment with etoposide ($P = 0.1574$). shGPX4; GPX4-knockdown LCL-K cells.;*$P < 0.05$; n.s., non-significant

glutathione. DLBCL is one of the cancer cell types that are highly sensitive to ferroptosis, for unknown reasons [39, 40]. If these observations also apply to our results, the poor prognosis of patients with GPX4 overexpression may be owing to suppression of ferroptosis. To determine whether our result is related to ferroptosis, we would need to verify whether cell death rate increases under treatment with GPX4 inhibitors such as ferrostatin-1 and vitamin E [40] or GPX4-inhibitory peptide [41]. Though many aspects of ferroptosis remain unexplained, such as the execution factor and the substances detected downstream [40], these reports suggest that GPX4 is unique and different from other antioxidants. GPX4 has the potential to become a new therapeutic target as research on GPX4 advances, with the elucidation of the structure of GPX4, for example ref. [41].

In conclusion, we demonstrate that GPX4 overexpression is associated with poor prognosis in patients with DLBCL and GPX4 overexpression decreases ROS-induced cell death *in vitro* in LCL-K cells. Although several questions, such as the mechanism of the overexpression of GPX4, remain unsolved, and prospective studies must be performed with regard to potential clinical applications, GPX4 has the potential to become a novel anticancer drug target, as well as a prognostic predictor.

Acknowledgements This work was supported in part by a Grant-in-Aid from the Ministry of Education, Culture, Sports, Science, and Technology of Japan (No. 21790345).

Conflict of interest The authors declare that they have no conflict of interest.

References

1. Swerdlow SH, Campo E, Harris NL, et al. WHO classification of tumours of haematopoietic and lymphoid tissues, 4th edn. Lyon, France: IARC; 2008.
2. Swerdlow SH, Campo E, Pileri SA, et al. The 2016 revision of the World Health Organization classification of lymphoid neoplasms. Blood. 2016;127:2375–2390.
3. Hu S, Xu-Monette ZY, Balasubramanyam A, et al. CD30 expression defines a novel subgroup of diffuse large B-cell lymphoma with favorable prognosis and distinct gene expression signature: a report from the International DLBCL Rituximab-CHOP Consortium Program Study. Blood. 2013;121:2715–2724.

4. Ennishi D, Takeuchi K, Yokoyama M, et al. CD5 expression is potentially predictive of poor outcome among biomarkers in patients with diffuse large B-cell lymphoma receiving rituximab plus CHOP therapy. Ann Oncol. 2008;19:1921–1926.
5. Yamaguchi M, Seto M, Okamoto M, et al. De novo CD5+ diffuse large B-cell lymphoma: a clinicopathologic study of 109 patients. Blood. 2002;99:815–821.
6. Lincoln DT, Ali Emadi EM, Tonissen KF, et al. The thioredoxin-thioredoxin reductase system: over-expression in human cancer. Anticancer Res. 2003;23:2425.
7. Jan L, Sandra JH, Ying H, et al. The cystine/glutamate antiporter system x(c)(-) in health and disease: from molecular mechanisms to novel therapeutic opportunities. Antioxid Redox Signal. 2013;18:522–555.
8. Le J, Ning K, Tongyuan L, et al. Ferroptosis as a p53-mediated activity during tumour suppression. Nature. 2015;520:557.
9. Gandin V, Fernandes AP, Rigobello MP, et al. Cancer cell death induced by phosphine gold(I) compounds targeting thioredoxin reductase. Biochem Pharmacol. 2010;79:90–101.
10. Chao Y, Biehuoy S, Philip R, et al. Potent activity of indolequinones against human pancreatic cancer: identification of thioredoxin reductase as a potential targaet. Mol Pharmacol. 2009;76:163–172.
11. Tobe R, Yoo MH, Fradejas N, et al. Thioredoxin reductase 1 deficiency enhances selenite toxicity in cancer cells via a thioredoxin-independent mechanism. Biochem J. 2012;445:423–430.
12. Seiler A, Schneider M, Förster H, et al. Glutathione peroxidase 4 senses and translates oxidative stress into 12/15-lipoxygenase dependent- and AIF-mediated cell death. Cell Metab. 2008;8:237–248.
13. Wortmann M, Schneider M, Pircher J, et al. Combined deficiency in glutathione peroxidase 4 and vitamin E causes multiorgan thrombus formation and early death in mice. Circ Res. 2013;113:408–417.
14. Yant LJ, Ran Q, Rao L, et al. The selenoprotein GPX4 is essential for mouse development and protects from radiation and oxidative damage insults. Free Radic Biol Med. 2003;34:496–502.
15. Yagublu V, Arthur JR, Babayeva SN, et al. Expression of selenium-containing proteins in human colon carcinoma tissue. Anticancer Res. 2011;31:2693.
16. Guerriero E, Capone F, Accardo M, et al. GPX4 and GPX7 over-expression in human hepatocellular carcinoma tissues. Eur J Histochem. 2015;59:2540.
17. Liu J, Du J, Zhang Y, et al. Suppression of the malignant phenotype in pancreatic cancer by overexpression of phospholipid hydroperoxide glutathione peroxidase. Hum Gene Ther. 2006;17:105–116.
18. Cejas P, García-Cabezas MA, Casado E, et al. Phospholipid hydroperoxide glutathione peroxidase (PHGPx) expression is downregulated in poorly differentiated breast invasive ductal carcinoma. Free Radic Res. 2007;41:681–687.
19. Rudenko E, Kondratov O, Gerashchenko G, et al. Aberrant expression of selenium-containing glutathione peroxidases in clear cell renal cell carcinomas. Exp Oncol. 2015;37:105.
20. Van Blarigan EL, Ma J, Kenfield SA, et al. Plasma antioxidants, genetic variation in SOD2, CAT, GPX1, GPX4, and prostate cancer survival. Cancer Epidemiol Biomark Prev. 2014; 23:1037–1046.
21. Lan X, Xing J, Gao H, et al. Decreased expression of selenoproteins as a poor prognosticator of gastric cancer in humans. Biol Trace Elem Res. 2017;178:22–28.
22. Hans CP, Weisenburger DD, Greiner TC, et al. Confirmation of the molecular classification of diffuse large B-cell lymphoma by immunohistochemistry using a tissue microarray. Blood. 2004;103:275–282.
23. Yoshimori M, Imadome K-I, Komatsu H, et al. CD137 expression is induced by Epstein–Barr virus infection through LMP1 in T or NK cells and mediates survival promoting signals. PLoS ONE. 2014;9:e112564.
24. Hafer K, Schiestl RH. Biological aspects of dichlorofluorescein measurement of cellular reactive oxygen species. Radiat Res. 2008;170:408.
25. Grinberg YY, van Drongelen W, Kraig RP. Insulin-like growth factor-1 lowers spreading depression susceptibility and reduces oxidative stress. J Neurochem. 2012;122:221–229.
26. Bhattacharya S, Gachhui R, Sil PC. Hepatoprotective properties of kombucha tea against TBHP-induced oxidative stress via suppression of mitochondria dependent apoptosis. Pathophysiology. 2011;18:221–234.
27. Vessey DA, Lee KH, Blacker KL. Characterization of the oxidative stress initiated in cultured human keratinocytes by treatment with peroxides. J Invest Dermatol. 1992;99: 859–863.
28. Ueta T, Inoue T, Furukawa T, et al. Glutathione peroxidase 4 is required for maturation of photoreceptor cells. J Biol Chem. 2012;287:7675–7682.
29. Imai H, Suzuki K, Ishizaka K, et al. Failure of the expression of phospholipid hydroperoxide glutathione peroxidase in the spermatozoa of human infertile males1. Biol Reprod. 2001; 64:674–683.
30. Imai H, Hirao F, Sakamoto T, et al. Early embryonic lethality caused by targeted disruption of the mouse PHGPx gene. Biochem Biophys Res Commun. 2003;305:278–286.
31. Roveri A, Maiorino M, Ursini F. Enzymatic and immunological measurements of soluble and membrane-bound phospholipid-hydroperoxide glutathione peroxidase. Methods Enzymol. 1994;233:202–212.
32. Uhlen M, Fagerberg L, Hallstroem BM, et al. Tissue-based map of the human proteome. Science. 2015;347:394.
33. Brown KM, Pickard K, Nicol F, et al. Effects of organic and inorganic selenium supplementation on selenoenzyme activity in blood lymphoctyes, granulocytes, platelets and erythrocytes. Clin Sci. 2000;98:593.
34. Boulon S, Westman BJ, Hutten S, et al. The nucleolus under stress. Mol Cell. 2010;40:216–227.
35. Peroja P, Pasanen AK, Haapasaari KM, et al. Oxidative stress and redox state-regulating enzymes have prognostic relevance in diffuse large B-cell lymphoma. Exp Hematol Oncol. 2012;1:2.
36. Harris IS, Brugge JS. Cancer: the enemy of my enemy is my friend. Nature. 2015;527:170–1.
37. Andreadis C, Gimotty PA, Wahl P, et al. Members of the glutathione and ABC-transporter families are associated with clinical outcome in patients with diffuse large B-cell lymphoma. Blood. 2007;109:3409–3406.
38. DeNicola GM, Karreth FA, Humpton TJ, et al. Oncogene-induced Nrf2 transcription promotes ROS detoxification and tumorigenesis. Nature. 2011;475:106–109.
39. Yang Wan S, SriRamaratnam R, Welsch Matthew E, et al. Regulation of ferroptotic cancer cell death by GPX4. Cell. 2014;156:317–331.
40. Cao JY, Dixon SJ. Mechanisms of ferroptosis. Cell Mol Life Sci. 2016;73:2195–2209.
41. Sakamoto K, Sogabe S, Kamada Y, et al. Discovery of GPX4 inhibitory peptides from random peptide T7 phage display and subsequent structural analysis. Biochem Biophys Res Commun. 2017;482:195–201.